



TOWARDS A FULL DIGITAL APPROACH FOR AEROACOUSTICS EVALUATION OF AUTOMOTIVE ENGINE COOLING FANS AND HVAC BLOWERS

Vincent LE GOFF¹, Benoit LE HENAFF²,
Mélanie PIELLARD², David PIHET², Bruno COUTTY²

¹ *Exa Corporation, Burlington, MA, 01803, USA*

² *Delphi Thermal Systems, Bascharage, L-4940, Luxembourg*

SUMMARY

This paper focuses on the prediction of an automotive Heating Ventilating and Air Conditioning (HVAC) module blower using a three-dimensional compressible and unsteady Computational Fluid Dynamics (CFD) solver based on the Lattice-Boltzmann Method (LBM). Experimental method and results are described and analyzed. The numerical approach is presented and simulation results are compared to experiments. Acoustic Overall Sound Power Level computed between 100 Hz and 5000 Hz is predicted within 0.5 dB from experiments, showing an excellent agreement. Transient and spectral simulation results are analyzed to bring more understanding on the main flow-induced noise source generation mechanisms.

INTRODUCTION

In the automotive industry, the reduction of the main noise contributors of passenger cars such as engine, rolling, and aerodynamic noise, is giving more and more value to the acoustic efficiency of components and subsystems. This is particularly true with rotating machines, such as engine cooling fans and Heating Ventilating and Air Conditioning (HVAC) module blowers. Since they can represent a strong competitive advantage and be a real market differentiator, automotive suppliers have to address the products' acoustic performances as early as possible in the development phase.

Experimental methods have been used historically to reduce the most obvious noise sources and led to acoustically efficient products. But they have also shown limitations such as time, cost of prototypes, mechanical and aerodynamic constraints. In addition, the targets specified by car manufacturers are becoming harder to achieve. When dealing with experiments, the lack of insight into acoustic phenomena can reduce innovation opportunities. With the decreasing cost of computational resources, using a digital approach could help go beyond these constraints, reduce

the number of expensive prototypes, accelerate the products development cycles, and bring more understanding in the noise generation mechanisms. Integrating these methods in the current development process of fan and blower systems could lead to achieving better acoustic performance and even exceeding the present targets while, at the same time, managing aerodynamic and mechanical objectives.

In a first publication [1], it has been shown how PowerFLOW, a compressible and unsteady CFD solver based on the Lattice-Boltzmann Method, can accurately capture the flow induced noise phenomena at the origin of the broadband contributions of a Condenser Radiator Fan Module (CRFM). The method has been successfully used to rank different fan designs upon their aeroacoustic performance. A more recent study [2] presented its accuracy at predicting the tonal noise radiated by such a fan but also the effect of an upstream geometry on broadband noise.

The overall accuracy achieved on predicting both broadband and tonal noise for these two configurations gives confidence in the use of simulation results to understand the flow features at the origin of the noise. It makes this approach powerful to evaluate design changes quickly during the development phase and to understand their impact on the noise sources, leading to better aeroacoustic performance.

As for CRFM products, the implementation of such an approach to HVAC modules could help go beyond acoustic targets and provide a real advantage over market competitors. This paper focuses on the first phase of this implementation, i.e. the numerical evaluation of flow-induced noise radiated by HVAC blowers using a Lattice-Boltzmann Method. In a first section the strategy for validating the prediction of the aeroacoustic performance of HVAC modules will be presented. The second section will focus on the experimental setup and results. The numerical approach will be described in a third section. Simulation and experimental results will be compared in the fourth section. Transient and spectral simulation results will be analyzed to get an insight on the flow-induced noise mechanisms at the origin of the main noise sources.

HVAC MODULE NOISE VALIDATION STRATEGY

The goal of the present study is to validate the possibility of using simulation results to predict the aeroacoustic performance of an HVAC module. When comparing experimental and simulation results many factors can interfere. In particular, the differences between the exact geometry of the tested product compared to its nominal Computer-Aided Design (CAD) representation are a source of uncertainty. A complete HVAC module comprises a significant number of parts, some of them with a variable position (flaps, vents ...), making the comparison between a real system and a digital model challenging. Therefore, and because aeroacoustic phenomena are significantly impacted by small geometry details, using a subsystem approach for validating a numerical method could help reduce these uncertainties. The first phase of this validation study will focus on the prediction of an HVAC module blower mounted on a simplified bench. The HVAC blower used in this study consists of a centrifugal wheel rotating in a scroll and blowing into a diffuser expansion. Wheel rotation is ensured by an electric motor.

The automotive HVAC module blower chosen for this first validation phase is a production part from Delphi Thermal Systems. The advantage of using a production part is that the manufacturing process is robust and geometrical tolerances are much lower than on prototypes. In addition, the CAD representation of this part contains all geometrical details, including the cooling channel and its interaction with the motor rotor. To facilitate the comparisons, a specific, easy to model, experimental bench has been developed to measure the acoustic power radiated by the blower.

EXPERIMENTAL METHOD

Experimental setup

The experimental set-up is the ISO 10302 [3] set-up, usually used to evaluate acoustic power generated by fans, without Mylar plenum. The HVAC module blower used in this study comprises a 150 mm diameter wheel with 39 blades rotating in its corresponding scroll. Fan rotation is ensured by an electric motor rotating at 2500 Rotation Per Minute (RPM). A standard diffuser is attached at the outlet of the scroll and the system is mounted on a simplified wood support as presented in Figure 1. The whole bench is placed in a semi anechoic room, part of Delphi Thermal Systems. Ten equally spaced microphones are placed on a 2 meters radius hemi sphere centered on the bench; they are used to record pressure histories and compute Sound Pressure Levels (SPLs) and the acoustic power level L_w .

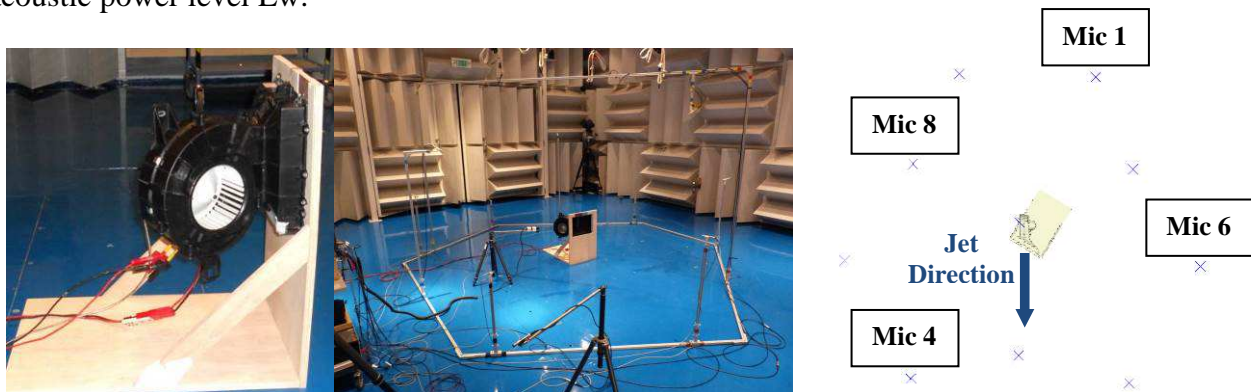


Figure 1: Left: Experimental setup. Right: Microphone positions seen from top.

Experimental results

The acoustic power spectrum is computed from pressure histories recorded on ten microphones and is plotted using a 2 Hz resolution frequency in Figure 2. The Blade Passing Frequency (BPF) peak at 1700 Hz is clearly visible on the spectrum but the main contributions to overall noise levels and acoustic power come from broadband noise. Four main humps in the spectrum are visible, between 400 Hz and 500 Hz, 800 Hz and 1000 Hz, 1300 Hz and 1650 Hz, and 1850 Hz and 2300 Hz.

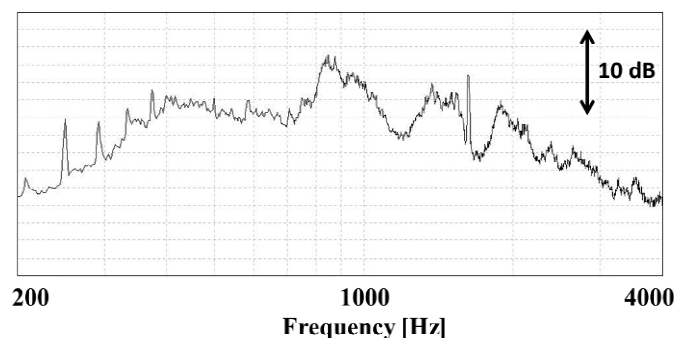


Figure 2: Experimental acoustic power spectrum.

The spectrogram computed between 1000 RPM and 3000 RPM shown in Figure 3 confirms that these contributions are not correlated with the rotational speed of the blower. The highest noise level is located in the second hump at 840 Hz, and is even higher than the BPF peak. It appears difficult to give an explanation on the particular phenomenon occurring at this frequency using these experimental data only. Simulation results could help to understand and reduce the flow features at the origin of this contribution.

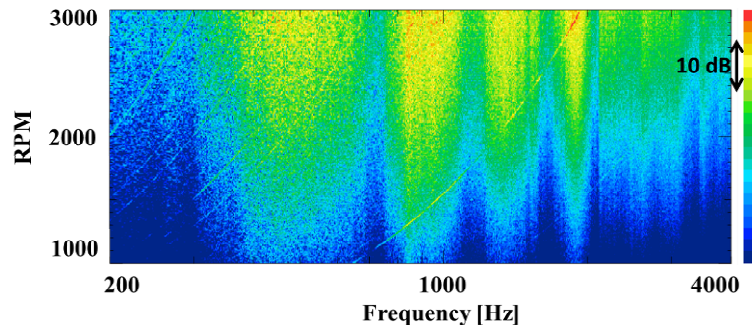


Figure 3: Experimental acoustic power spectrogram between 1000 RPM and 3000 RPM.

Because performing a three-dimensional unsteady simulation of a rotating blower for a physical time comparable to experiments would not be possible in a typical development cycle, the effect of using short pressure signals to compute acoustic power levels has to be assessed. A time interval analysis using a short signal representative of affordable simulation signals is performed on the experimental pressure histories. For each microphone, 20 intervals spanned over the experimental signal are used to compute SPLs. The corresponding acoustic power spectra are computed in one-third octave bands from 100 Hz to 5000 Hz. For each time interval and each third octave frequency band, the results are compared to the original acoustic power spectrum using the whole pressure signal. The delta between short signal spectra and the original spectrum are reported in the spectrogram plotted in Figure 4.

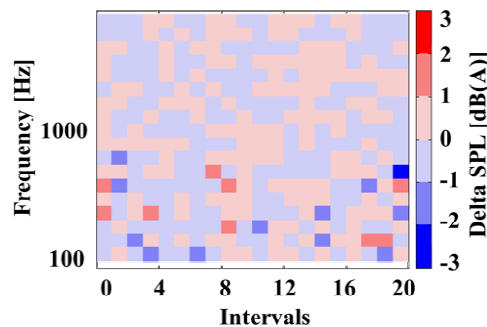


Figure 4: Variation of acoustic power third octave band levels in time using short time intervals at 2500 RPM.

It appears that the most significant noise level variations are observed for low frequencies, i.e. below 800 Hz. This was expected as third octave frequency band levels are computed by summing the narrow frequency band levels from a previous Fast Fourier Transform (FFT) spectrum in the considered frequency range. The lower and narrower third octave bands being computed using less FFT narrow bands, more statistical variation is introduced. Considering all frequency bands, the maximum variation is about -2 dB, occurring at 400 Hz for interval 20. Considering the frequency band containing the BPF, the maximum variation is about -0.6 dB for interval 10. Finally, comparing the OASPL integrated between 100 Hz and 5000 Hz, the maximum delta is about 0.4 dB for interval 16.

The same analysis is performed on six rotational speeds between 1000 RPM and 3500 RPM. The maximum variations considering all frequency bands, the frequency band containing the BPF and the OASPL are reported as functions of the rotational speed in Figure 5. Except for very low rotational speed, the maximum difference observed in one band of third octave acoustic power spectrum from 100 Hz to 5000 Hz using a short pressure signal is between 2 dB and 3 dB (blue straight line). As the maximum variation often occurs at the lowest frequencies, the same analysis is performed excluding the third octave bands between 100 Hz and 200 Hz. The maximum variations are then very stable, around 2 dB (blue dashed line). Considering the frequency band containing the BPF and the OASPL value, the maximum variation seems stable over the rotational speed, about 1 dB and 0.3 dB respectively.

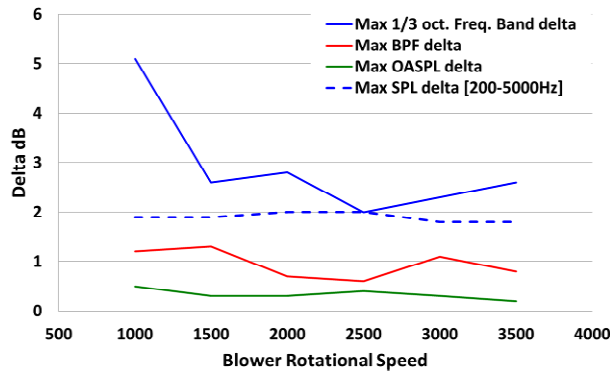


Figure 5: Maximum acoustic power variation using short intervals compared to using the whole experimental signal.

Whereas experimental results variations may not fully reflect what is observed in simulations results, it is to be expected that the analysis of short simulation signals could affect the robustness of the results at low frequencies.

NUMERICAL METHOD

Lattice-Boltzmann Method (LBM)

The compressible and unsteady Computational Fluid Dynamics (CFD) / Computational AeroAcoustics (CAA) solver PowerFLOW 5.0b used for this study is based on the Lattice Boltzmann Method (LBM). Unlike conventional methods based on discretizing the macroscopic continuum equations, LBM starts from “mesoscopic” kinetic equations, i.e. the Boltzmann equation, to predict macroscopic fluid dynamics. Whereas resolvable flow scales can be simulated using this approach, the unresolved small scales are modelled by replacing the molecular relaxation time scale of the Boltzmann equation with an effective turbulent relaxation time scale derived from a systematic Renormalization Group procedure detailed by Chen *et al.* [4] and Chen [5].

The LBM scheme is solved on a Cartesian grid, which cubic elements are called voxels. Their sizes are defined in Variable Resolution (VR) regions, the voxel size changing by a factor of two from one VR region to an adjacent VR region. Prior to the simulation, discretization in space is performed automatically based on these VR regions. Intersections of the voxels with the blower surface mesh produce surface elements called surfels. These elements are used during the simulation to handle the interactions between solid parts and adjacent fluid regions.

For simulation of flow with arbitrary geometry rotating in time around a fixed axis, the 3-D computational domain is divided into an inner and an outer domain. The inner domain has a grid attached to the rotating geometry so that the geometry does not have a relative motion with respect to the grid. This forms a “body-fixed” Local Reference Frame (LRF) domain with the rotating geometry. The grid in the outer domain is fixed with the ground and forms a “ground-fixed” reference frame domain. Between the inner domain and the outer domain, a closed transparent interface connects the fluid regions. Details related to the implementation of the interface region between the inner and the outer region are given by Zhang *et al.* [6]. This method was also recently used by Mann *et al.* [7], Pérot *et al.* [8-10], Lee *et al.* [11] for predicting and validating fan and HVAC systems performance.

Numerical model

Because the HVAC blower used in this study is a production part from Delphi Thermal Systems, the available CAD data for the entire system (wheel, scroll, electric motor and diffuser) was already very detailed. All geometrical information and details have been kept during the preparation of the

surface mesh. In order to get even closer to the real part, additional details have been manually added to the existing CAD model based on observations and measurements. In particular, the fan counter-weights have been measured and added to the wheel geometry, taking into account each balancing counter-weight, as well as some plastic injection points.

The specifically developed wood support is also modeled and the whole system is placed in a large simulation domain. As in experiments the rotational speed of 2500 RPM is imposed in the simulation. Pressure boundary conditions are applied to the boundary of the simulation domain and atmospheric pressure is imposed. The simulation domain includes sponge zones to avoid any spurious reflections of acoustic waves from the boundary conditions. 11 variable resolution regions are defined in the simulation domain. Specific regions are defined in the vicinity of the blower to capture all flow-induced phenomena at the origin of the noise, as presented in Figure 6. The chosen finest voxel size allows a proper representation of the finest geometry details. Local resolution at microphones location is set to ensure the propagation of acoustic waves using more than 16 points per wavelength at 5 kHz [12]. A few rotations of the wheel are simulated. Time-domain convergence of flow and noise is reached after two complete fan revolutions, and flow and acoustics records start at this time.

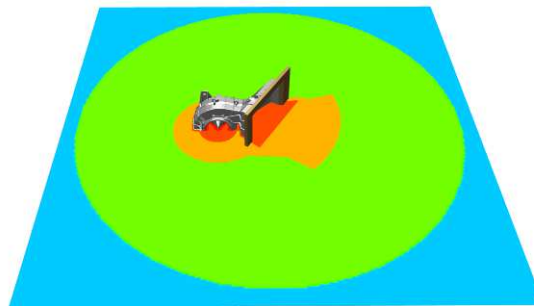


Figure 6: Resolution regions in the vicinity of the blower.

ACOUSTIC POWER PREDICTIONS

Direct Propagation

The strength of three-dimensional unsteady and compressible simulations based on LBM is the capability to recover simultaneously the flow and the corresponding acoustic fields. Acoustic waves generated in the source regions are propagated to the far-field and pressure histories are recorded directly at the microphones locations in the simulation. Experimental and simulation acoustic power levels are derived from the SPLs computed on the ten microphones, and compared in Figure 7.

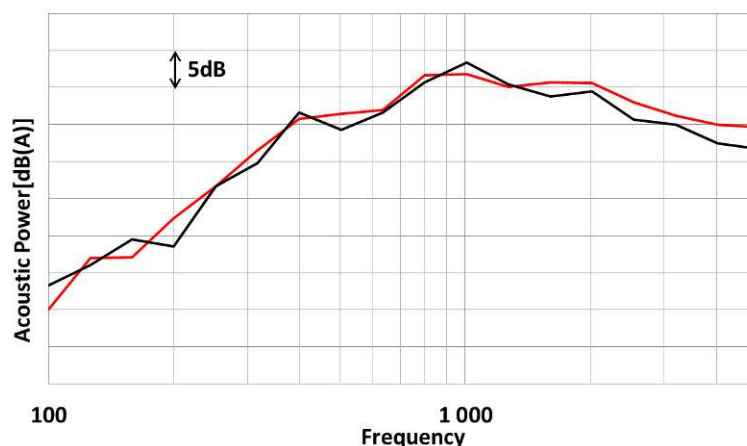


Figure 7: One-third octave bands Acoustic Power. — Experiments. — Simulation (direct).

With predictions showing a ± 2 dB accuracy per third octave bands, a good agreement is observed between experimental and simulated acoustic power levels between 250 and 1250 Hz. More variations are visible in the lower frequency range, i.e. below 250 Hz. This could be explained by the effects of using short signals for the FFT processing of simulation results. Above 1250 Hz, the predicted results are underestimated by 2 to 3 dB. In order to better understand this underestimation, SPLs obtained on four microphones are compared in Figure 8; their location is shown in Figure 1.

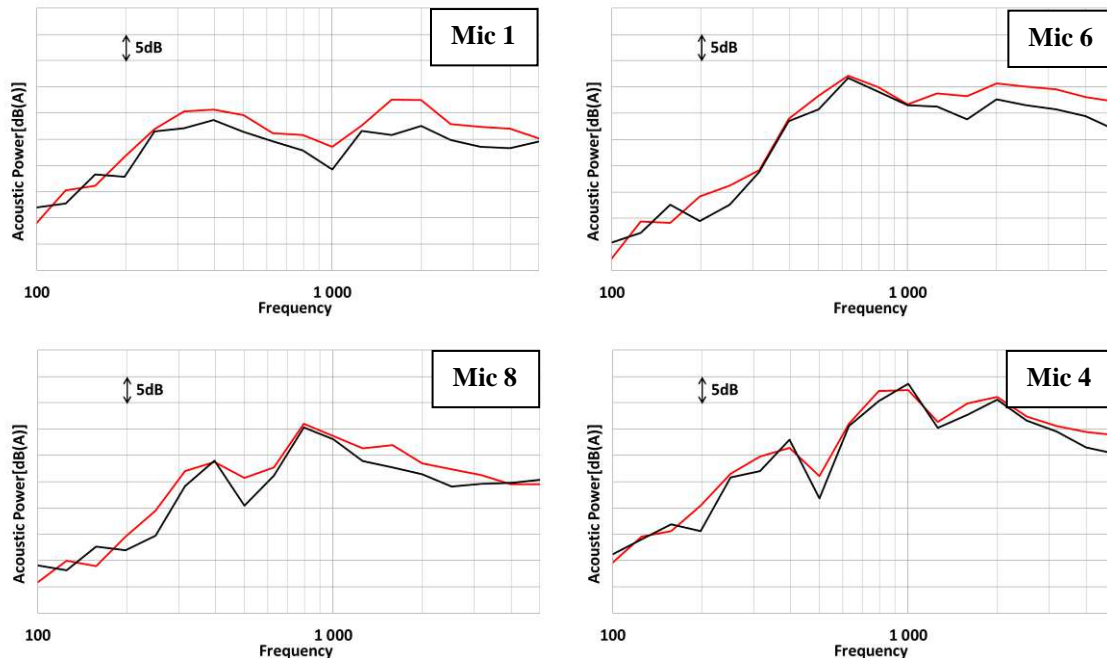


Figure 8: One-third octave bands SPLs. — Experiments. — Simulation (direct).

The analysis of SPLs points toward a dependency of prediction on microphones location. The underestimation of simulation results at high frequencies appears even stronger for microphones 1 and 6 on the opposite side of the jet. The predictions are slightly better for microphone 8 on the side of the blower. Microphone 4 on the jet side shows a good accuracy up to 3 kHz.

As a good accuracy is achieved on the jet side, the simulation is able to recover the flow-induced noise sources up to 3 kHz. But the direct propagation of these sources to far field microphones at 2 meters on the opposite side of the jet presents some limitations. To check these propagation effects, an acoustic propagation solver based on a Ffowcs-Williams and Hawkings (FW-H) method is used to recover the pressure histories at the microphones location based on the pressure, velocity and density information of a virtual reference sphere surrounding the blower and its support.

FW-H method

Although PowerFLOW has intrinsic CAA capabilities and can compute the noise directly from unsteady flow simulations, in order to compute the noise at far-field microphone locations, an integral extrapolation method based on an acoustic analogy can be used. In this case, this method will help verifying any direct propagation limitation on the opposite side of the jet. An integral solver based on the forward-time resolution of the FW-H equation based on Farassat's formulation 1a [13] is employed. Details about the formulation are given in [14]-[16]. The “porous” formulation [14] uses a permeable (transparent) surface, on which pressure, density, and the three velocity components are recorded and used as input. This formulation is particularly useful to take any diffraction or screening effects into account. To account for ground reflections, an image method is used. In this case, a transparent sphere comprising the blower and most of the bench is used as the permeable surface, as shown in Figure 9a. Pressure histories are calculated at microphone locations using this method and acoustic power levels are derived from the SPLs. The comparison of

experimental results, simulation results using direct propagation and simulation results using FW-H method is plotted in Figure 9b.

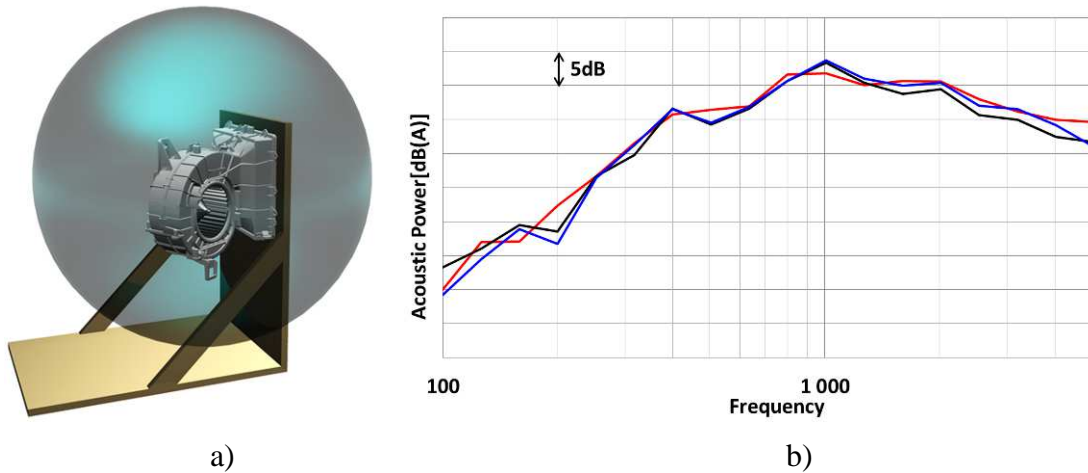


Figure 9: a) Reference sphere used for FW-H propagation as permeable surface.

b) One-third octave bands Acoustic Power. — Experiments. — Simulation (direct). — Simulation (FW-H).

Whereas predicted acoustic power levels using the direct approach or the FW-H method are very similar in the mid-frequency range (250-1250 Hz), the lower frequencies show slightly more variations. Again, this is most likely due to the use of short pressure signals for computing the FFT in the simulation. But the most significant change is the improvement of the high frequency levels. The predicted acoustic power spectrum using the FW-H method now shows a very good accuracy within 2 dB from experiments from 250 Hz up to 4 kHz.

The comparisons of experimental and predicted SPLs are presented in Figure 10. The comparison of predicted SPLs using the FW-H method and experimental results shows an overall better agreement. This is particularly the case at high frequencies and even more for microphones located on the opposite side of the jet. Very similar results are observed on the jet side, with some improvement on microphones 4 and 8.

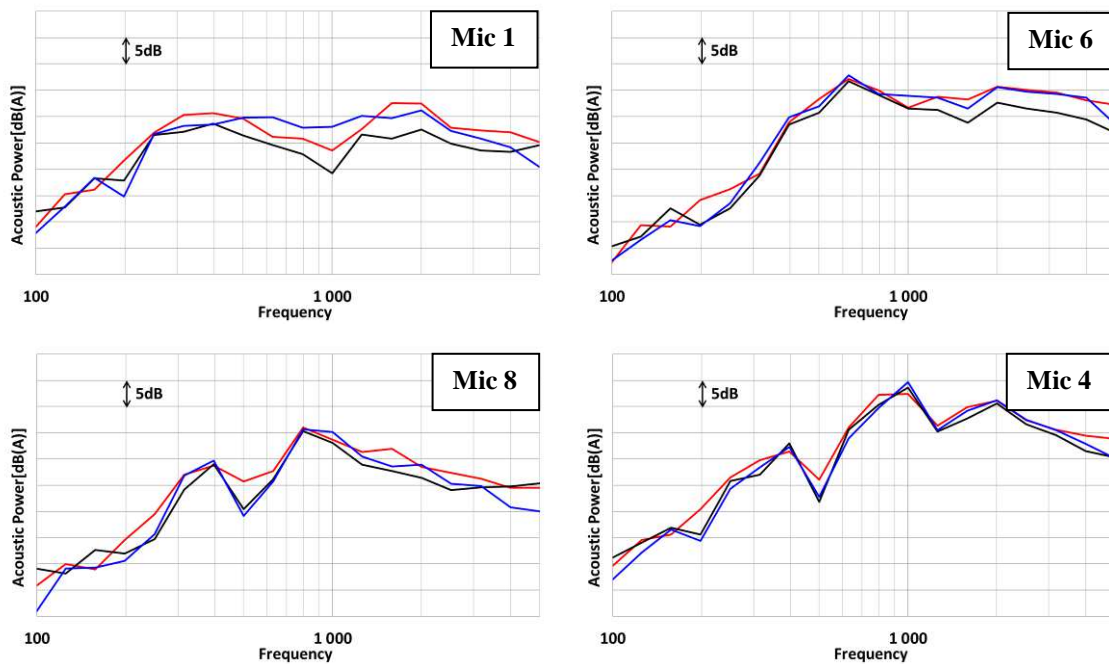


Figure 10: One-third octave bands SPLs. — Experiments. — Simulation (direct). — Simulation (FW-H).

This confirms that the use of an alternative propagation method is helping pushing the limitations of using the direct approach with microphones as far as two meters from the source. The resolution used between the source regions and the microphones appears to be not sufficient to directly propagate the acoustic waves without noticeable dissipation. However the accuracy achieved using a FW-H method shows that the noise generation mechanisms are captured properly in the simulation.

The predicted acoustic power now shows a ± 2 dB accuracy on each third octave band between 250 Hz and 4 kHz. Simulation results can then be used with confidence to better understand the flow induced phenomena at the origin of the noise.

INSIGHT ON MAIN NOISE SOURCES

Looking at the acoustic power spectrum in narrow bands in Figure 11, it appears that the main noise contributors are located in the [750-1050] Hz frequency range.

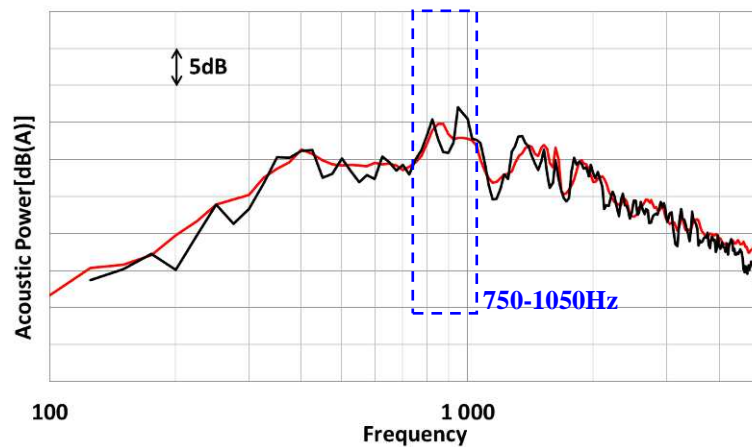


Figure 11: Narrow bands Acoustic Power spectrum ($\Delta\text{Hz} = 25$ Hz). — Experiments. — Simulation (FW-H).

As this frequency range shows the highest noise levels, and considering it is also perceived as annoying, it represents a real acoustic quality issue. Transient and spectral analysis of simulation results is focused on this frequency range to identify and understand the flow features at the origin of the noise.

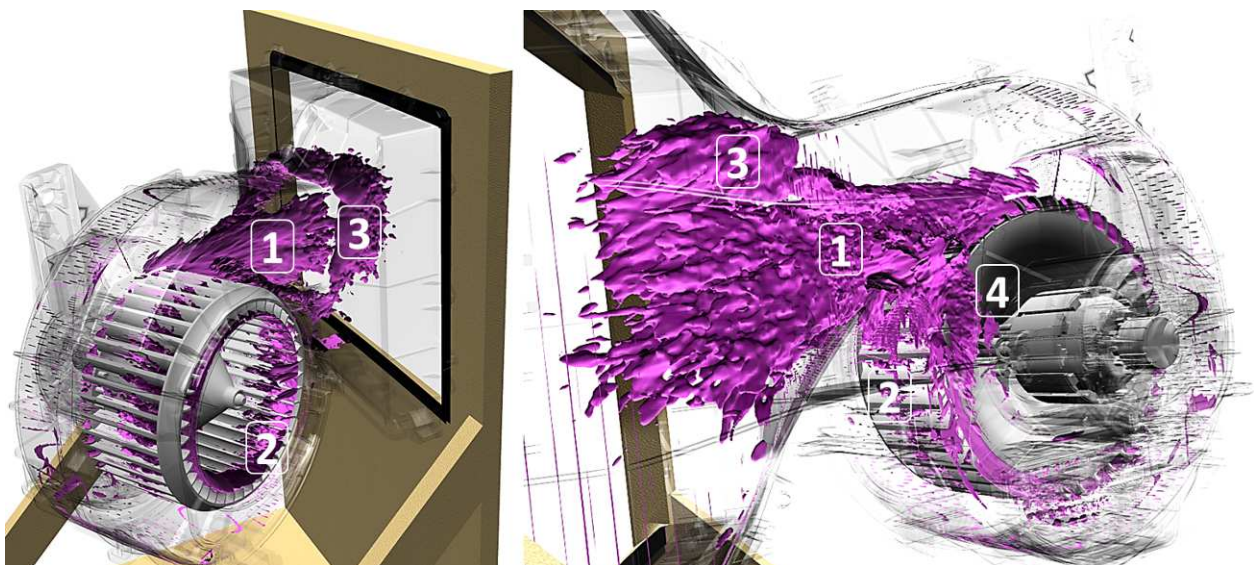


Figure 12: Isosurfaces of pressure fluctuations in dB, filtered in [750-1050] Hz.

Isosurfaces of pressure fluctuations filtered in [750-1050] Hz are plotted in Figure 12. Four main regions can be identified as showing the highest pressure fluctuations levels: the first one is located between the channel used for the motor cooling and the scroll cut-off to the middle of the diffuser, the second one at the inlet of the scroll, the third one in the diffuser, and the fourth one between the wheel and the scroll below the cut-off. Presenting a high level of pressure fluctuations, these regions are likely to be related the main noise sources in the considered frequency band.

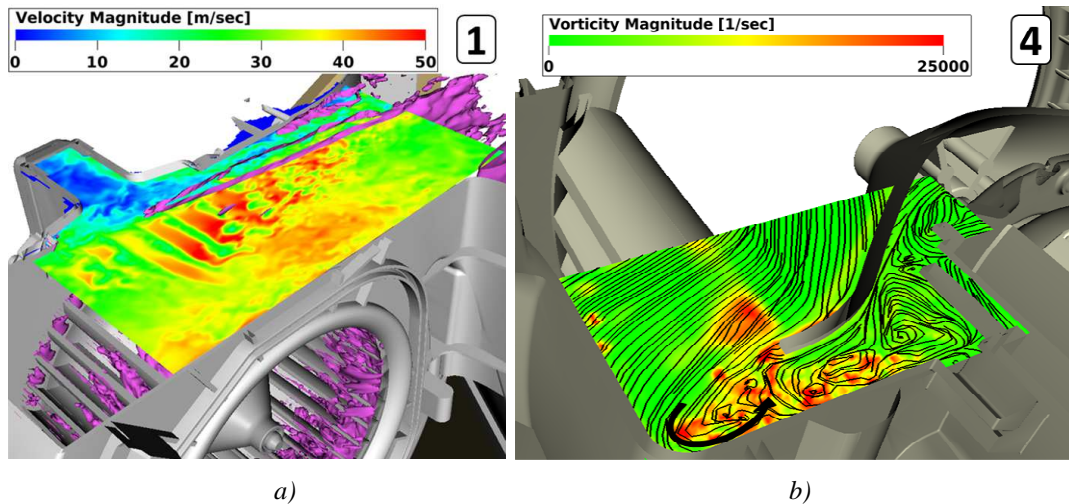


Figure 13: a) Instantaneous Velocity Magnitude on a horizontal plane. Pink: Isosurfaces of pressure fluctuations in dB, filtered in [750-1050] Hz.
b) Instantaneous Vorticity Magnitude on a horizontal plane.

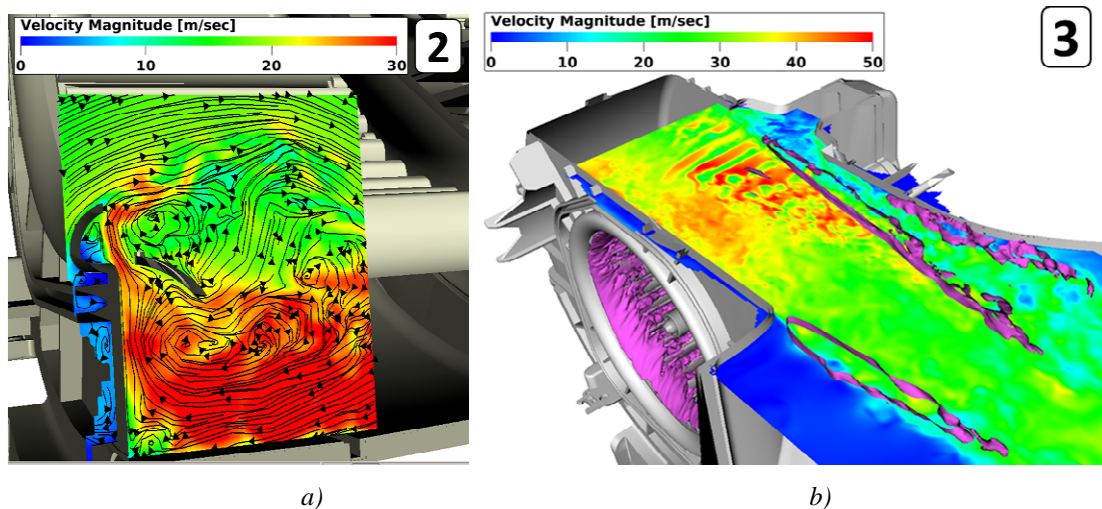


Figure 14: a) Instantaneous Velocity Magnitude on a vertical plane aligned with the wheel axis.
b) Instantaneous Velocity Magnitude on a horizontal plane.
Pink: Isosurfaces of pressure fluctuations in dB, filtered in [750-1050] Hz.

Figure 13a shows a snapshot of the velocity magnitude field on a horizontal plane passing through the cooling channel. High velocities corresponding to the flow going out of the wheel are observed. At the same height a large low velocity region is present at the entrance and in the cooling channel. When the flow comes out of the wheel and passes in front of the cooling channel, the velocity gradient creates a shear layer which is found to be the location of highest pressure fluctuations levels. Instantaneous vorticity magnitude is plotted on a horizontal plane below the cut-off in Figure 13b. In this region, when the flow comes out of the wheel, it faces the scroll wall at high speed. The space left between the wheel and the scroll is large and low pressured enough so that the flow spins around the wheel tip and a strong recirculation develops below the wheel hub.

Figure 14a presents a snapshot of the velocity magnitude field and the corresponding streamlines on a vertical plane aligned with the wheel axis. The pressure gradient between the outgoing and the incoming flow is creating a high velocity recirculation in the blower tip gap. This secondary flow is interacting with the clean incoming flow and a portion of it is impinging the wheel's blades. Instantaneous velocity magnitude in a horizontal plane above the scroll cut-off is shown in Figure 14b. The shape of the diffuser presents very steep angles in the side directions, making the flow detach immediately. The resulting shear layer is found to develop high pressure fluctuation levels in the considered frequency range. However, in a full HVAC module, a filter would be located just after the diffuser, and the flow behavior may slightly differ.

CONCLUSIONS

Based on the recent success of using a computational approach for the prediction of aeroacoustics performances of engine cooling fan modules, this paper focuses on the predictions of flow induced noise of HVAC blowers.

The acoustic power radiated by the system is measured at the acoustic facilities of Delphi Thermal Systems. Experimental results are presented and analyzed. A statistical study showed that using short pressure signals implies up to 3dB of statistical variations in the computation of the acoustic power lowest third octave bands over time.

A three-dimensional compressible and unsteady computational approach based on the Lattice-Boltzman Method is applied to recover simultaneously the turbulent flow and the corresponding acoustic field of the rotating blower in a semi anechoic environment. Whereas this direct approach shows a good agreement with experiments, with 2 dB accuracy per third octave bands between 250 Hz and 2 kHz, the higher frequencies are underestimated by the simulation. Microphone SPLs show that this statement depends on microphone locations and highlight a possible dissipation effect on the high frequencies.

An alternative propagation method based on a Ffowcs-Williams and Hawkings approach is used to predict the pressure histories at the microphone locations based on fluid information on a reference surface. The derived acoustic power spectrum shows much better predictions at high frequencies, especially on the opposite side of the jet. It confirms that the resolution scheme in this case does not seem appropriate for direct propagation of acoustic waves at high frequencies on microphones located two meters away from the source. With 2 dB accuracy up to 4 kHz, this study also confirms that the simulation captures all the aeroacoustic phenomena in this frequency range and that it can be used to understand and reduce the main flow-induced noise sources.

The analysis of aerodynamic pressure fluctuations in the flow field filtered in the frequency range [750-1050] Hz highlights four regions having significantly higher levels. Transient analyses are provided to give a better understanding of the flow features responsible for these high levels. The cooling channel, the axial distance of the wheel to the scroll, the tip gap shape and the diffuser angles are likely to play a significant role in these phenomena. This is an indication of the possible noise sources' location, which should be further confirmed by additional analyses.

The first phase of this validation study is completed. Additional parts from the complete HVAC module will be added in the next validation phases and the same computational approach will be evaluated.

BIBLIOGRAPHY

- [1] M. Piellard, B. Coutty, V. Le Goff, F. Pérot, V. Vidal – *Direct aeroacoustics simulation of automotive engine cooling fan system: an application study*, Aachen Acoustics Colloquium, Aachen, Germany, **2013**
- [2] M. Piellard, B. Coutty, V. Le Goff, F. Pérot, V. Vidal – *Direct aeroacoustics simulation of automotive engine cooling fan system: effect of upstream geometry on broadband noise*, 20th AIAA/CEAS Aeroacoustics Conference, Atlanta, GA, **2014**
- [3] ISO 10302: Acoustics – *Method for the measurement of airborne noise emitted by small air-moving devices*, **1996**
- [4] H. Chen, S. Orzag, I. Staroselsky, S. Succi – *Expanded analogy between Boltzmann Kinetic Theory of Fluid and Turbulence*, J. Fluid Mech., Vol 519, pp 301-314, **2004**
- [5] H. Chen – *Volumetric Formulation of the Lattice Boltzmann Method for Fluid Dynamics: Basic Concept*, Phys. Rev. E, Vol. 58, pp. 3955-3963, **1998**
- [6] R. Zang, Y. Li, C. Sun, R. Satti, R. Shock, J. Hoch, H. Chen – *Lattice Boltzmann approach for Local Reference Frames*, Communications in Computational Physics, 9, pp. 1193-1205, **2011**.
- [7] A. Mann, F. Pérot, M.S. Kim – *Advanced Noise Control Fan Direct Aeroacoustics Predictions using a Lattice Boltzmann Method*, 17th AIAA/CEAS Aeroacoustics Conference, Colorado Springs, USA, **2012**
- [8] F. Pérot, M.S. Kim, S. Moreau, D. Neal – *Investigation of the Flow Generated by an Axial 3-Blade Fan*, 13th ISROMAC Conference, 2010-082, Honolulu, Hawaii, **2010**.
- [9] F. Pérot, M.S. Kim, K. Wada, K. Norisada, M. Kitada, S. Hirayama, M. Sakai, S. Imahigasi, N. Sasaki – *HVAC blower aeroacoustics predictions based on the Lattice Boltzmann Method*, AJK Conference, AJK2011-23018, Hamamatsu, Japan, **2011**.
- [10] F. Pérot, M.-S. Kim, V. Le Goff, X. Carniel, Y. Goth, C. Chassaingon – *Numerical optimization of the tonal noise of a backward centrifugal fan using a flow obstruction*, Noise Control Engr. J., 61, 3, May-June, **2013**
- [11] D. Lee, F. Pérot, K-D. Ih, D. Freed – *Predictions of flow-induced noise of automotive HVAC systems*, SAE Technical Paper 2011-01-0493, **2011**
- [12] G. A. Brès, F. Pérot, D. Freed – *Properties of the Lattice Boltzmann Method for Acoustics*, 15th AIAA/CEAS Aeroacoustics Conference, Miami, FL, **2009**
- [13] F. Farassat, G. P. Succi – *The Prediction of Helicopter Discrete Frequency Noise*, Vertica, Vol. 7, No. 4, pp. 309-320, **1983**
- [14] G. A. Brès, F. Pérot, D. Freed – *A Ffowcs Williams-Hawkings Solver for Lattice Boltzmann Based Computational Aeroacoustics*, AIAA Paper 2010-3711, **2010**.
- [15] A. Naja-Yazdi, G. A. Brès, L. Mongeau – *An Acoustic Analogy Formulation for Moving Sources in Uniformly Moving Media*, Proceeding of the Royal Society of London A, Vol. 467(2125), pp. 144-165, **2011**
- [16] S. Noelting, M. Wessels, A. Keating, G. A. Brès – *Tandem cylinder noise predictions using a Lattice Boltzmann and Ffowcs Williams - Hawkings Methods*, AIAA 2010-3395, 14th AIAA/CEAS, Stockholm, Sweden, **2010**